

Neutron/proton ratio of nucleon emissions as a probe of neutron skin

X. Y. Sun^{a,b}, D. Q. Fang^a, Y. G. Ma^a, X. Z. Cai^a, J. G. Chen^a, W. Guo^a, W. D. Tian^a, H. W. Wang^a

^aShanghai Institute of Applied Physics, Chinese Academy of Sciences, Shanghai 201800, China

^bGraduate School of Chinese Academy of Sciences, Beijing 100039, China

Abstract

The dependence between neutron-to-proton yield ratio (R_{np}) and neutron skin thickness (δ_{np}) in neutron-rich projectile induced reactions is investigated within the framework of the Isospin-Dependent Quantum Molecular Dynamics (IQMD) model. The density distribution of the Droplet model is embedded in the initialization of the neutron and proton densities in the present IQMD model. By adjusting the diffuseness parameter of neutron density in the Droplet model for the projectile, the relationship between the neutron skin thickness and the corresponding R_{np} in the collisions is obtained. The results show strong linear correlation between R_{np} and δ_{np} for neutron-rich Ca and Ni isotopes. It is suggested that R_{np} may be used as an experimental observable to extract δ_{np} for neutron-rich nuclei, which is very significant to the study of the nuclear structure of exotic nuclei and the equation of state (EOS) of asymmetric nuclear matter.

Key words: isospin, neutron-proton ratio, neutron skin

Nuclear radius is one of the basic quantities of a nucleus. The proton root-mean-square (RMS) radius can be determined to very high accuracy via the charge radius measured by electromagnetic interactions, typically with an error of 0.02 fm or better for many nuclei [1]. In contrast, it is much more difficult to accurately determine the neutron density distribution of a nucleus experimentally [2]. Thus, the accuracy of experimental neutron radius is much lower than that of the proton radius. However, the information of neutron density is very important to the study of nuclear structure for neutron-rich nuclei, atomic parity non-conservation, iso-vector interactions, and neutron-rich matter in astrophysics etc. It is remarkable that a single measurement has so many applications in the research fields of atomic, nuclear and astrophysics [3, 4].

A nucleus with neutron number (N) being larger than proton number (Z) are expected to have a neutron skin (defined as the difference between the neutron and proton RMS radii: $\delta_{np} \equiv \langle r_n^2 \rangle^{1/2} - \langle r_p^2 \rangle^{1/2}$). The neutron skin thickness δ_{np} depends on the balance between various aspects of the nuclear force. The actual proton and neutron density distributions are determined by the balance between the isospin asymmetry and Coulomb force. δ_{np} is found to be related with a constraint on the equation of state (EOS) of asymmetric nuclear matter. Strong linear correlation between δ_{np} and L (the slope of symmetry energy coefficient C_{sym}), the ratio L/J (J is the symmetry energy coefficient at the saturation density ρ_0), $J - a_{sym}$ (a_{sym} is the symmetry energy coefficient of finite nuclei) are demonstrated [5]. This constraint is important for extrapolation of the EOS to high density and hence useful for studying properties of neutron star [5, 6, 7, 8, 9, 10, 11, 12]. Neutron skin thickness can yield a lot of information on the derivation of volume and surface symmetry energy, as well

Email addresses: dqfang@sinap.ac.cn (D. Q. Fang), ygma@sinap.ac.cn (Y. G. Ma)

as nuclear incompressibility with respect to density. δ_{np} is significant to the study of the EOS in different theoretical models such as Skyrme Hartree-Fock (SHF) [3, 4, 7, 8, 9, 11, 12], relativistic mean-field (RMF) [9, 10, 13], BUU model [14, 15, 16] and Droplet model [17]. Furthermore, neutron skin thickness helps to identify a nucleus with exotic structure. Thus the precise determination of δ_{np} for a nucleus becomes an important research subject in nuclear physics.

Several attempts have been made or suggested to determine the neutron density distribution such as using proton scattering, interaction cross sections in heavy ion collisions at relativistic energies [18], parity violating measurements [3, 4, 7, 8, 9], neutron abrasion cross sections in heavy ion collisions [19]. On the other hand, the neutron and proton transverse emission and double neutron-proton ratios have been studied as a sensitive observable of the asymmetry term of the nuclear EOS in the experiment [20] and different kinds of simulations [21, 22, 23, 24, 25]. In this Letter, the relationship between δ_{np} and the ratio of the emitted neutron and proton yields ($R_{np} = Y_n/Y_p$) in neutron-rich projectile induced reactions is, for the first time, presented within the framework of Isospin-Dependent Quantum Molecular Dynamics (IQMD) model. The possibility of extracting δ_{np} from R_{np} is investigated.

The QMD approach is a many-body theory that describes heavy-ion reactions from intermediate to relativistic energies [26]. It includes several important factors: initialization of the projectile and target, nucleon propagation in the effective potential, nucleon-nucleon (NN) collisions in a nuclear medium and the Pauli blocking effect. A general review of the QMD model can be found in [27]. The IQMD model is based on the QMD model with consideration of the isospin effect.

The dynamics of heavy ion collision at intermediate energies is governed mainly by three components: the mean field, two-body collisions, and Pauli blocking. Therefore, for an isospin-dependent reaction dynamics model, it is important to include isospin degrees of freedom with the above three components. In addition, the sampling of phase space of neutrons and protons in the initialization should be treated separately

because of the large difference between neutron and proton density distributions for nuclei that far from the β -stability line.

In the IQMD model, each nucleon i is represented by a Gaussian wave packet with definite width ($L = 2.16 \text{ fm}^2$) centered around the mean position and the mean momentum:

$$\Psi_i(\vec{\mathbf{R}}, t) = \frac{1}{(2\pi L)^{3/4}} \exp\left[-\frac{(\vec{\mathbf{R}} - \vec{\mathbf{R}}_i(t))^2}{4L}\right] \times \exp\left[\frac{i\vec{\mathbf{R}} \cdot \vec{\mathbf{p}}_i(t)}{\hbar}\right] \quad (1)$$

The nuclear mean field in the IQMD model is determined as following

$$U(\rho, \tau_z) = \alpha\left(\frac{\rho}{\rho_0}\right) + \beta\left(\frac{\rho}{\rho_0}\right)^\gamma + \frac{1}{2}(1 - \tau_z)V_c + C_{\text{sym}}\frac{(\rho_n - \rho_p)}{\rho_0}\tau_z + U^{\text{Yuk}} \quad (2)$$

with the normal nuclear matter density $\rho_0 = 0.16 \text{ fm}^{-3}$. ρ , ρ_n and ρ_p are the total, neutron and proton densities, respectively. τ_z is z -th component of the isospin degree of freedom, which equals 1 or -1 for neutron or proton, respectively. The coefficients α , β and γ are parameters for the nuclear EOS. C_{sym} is the symmetry energy strength due to the difference between neutron and proton. In the present work, we take $\alpha = -356 \text{ MeV}$, $\beta = 303 \text{ MeV}$ and $\gamma = 1.17$ which correspond to the so-called soft EOS with $C_{\text{sym}} = 32 \text{ MeV}$ and incompressibility of $K = 200 \text{ MeV}$. V_c is the Coulomb potential and U^{Yuk} is Yukawa (surface) potential. In the phase space initialization of the projectile and target, the density distributions of proton and neutron are distinguished from each other. The neutron and proton density distributions for the initial projectile and target nuclei in the present IQMD model are taken from the Droplet Model [28].

In the Droplet model, we can change the diffuseness parameter to get different density,

$$\rho_i(r) = \frac{\rho_i^0}{1 + \exp\left(\frac{r - C_i}{f_i t_i / 4.4}\right)}, i = n, p \quad (3)$$

where ρ_i^0 is the normalization constant which ensures that the integration of the density distribution equals to the number of neutrons ($i=n$) or protons ($i=p$); t_i

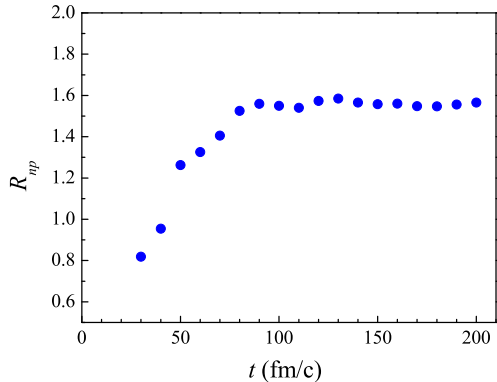


Figure 1: (Color online.) The evolution time dependence of R_{np} for $^{50}\text{Ca}+^{12}\text{C}$ at 50A MeV.

is the diffuseness parameter; C_i is the half density radius of neutron or proton determined by the Droplet model [28]

$$C_i = R_i[1 - (b_i/R_i)^2], i = n, p \quad (4)$$

here $b_i = 0.413f_it_i$, R_i is the equivalent sharp surface radius of neutron and proton. R_i and t_i are given by the Droplet model. A factor f_i is introduced by us to adjust the diffuseness parameter. In [29], Trzcińska et al. found that the half density radii for neutrons and protons in heavy nuclei are almost the same, but the diffuseness parameter for neutron is larger than that for the proton. So we introduce the factor f_i to adjust the diffuseness parameter for neutron. In the calculation for neutron-rich nucleus, $f_p = 1.0$ is used in Eq.(3) for the proton density distribution as in the Droplet model, while f_n in Eq.(3) is changed from 1.0 to 1.6. Different values of δ_{np} will be deduced from Eq.(3). Using the density distributions of the Droplet model, we can get the initial coordinate of nucleons in nuclei in terms of the Monte Carlo sampling method. The momentum distribution of nucleons is generated by means of the local Fermi gas approximation:

$$P_F^i(\vec{r}) = \hbar[3\pi^3\rho_i(\vec{r})]^{1/3}, (i = n, p) \quad (5)$$

In the IQMD model, the nucleon's radial density can be written as

$$\rho(r) = \sum \frac{1}{(2\pi L)^{3/2}} \exp\left(-\frac{r^2+r_i^2}{2L}\right) \frac{L}{2rr_i} [\exp\left(\frac{rr_i}{L}\right) - \exp\left(-\frac{rr_i}{L}\right)] \quad (6)$$

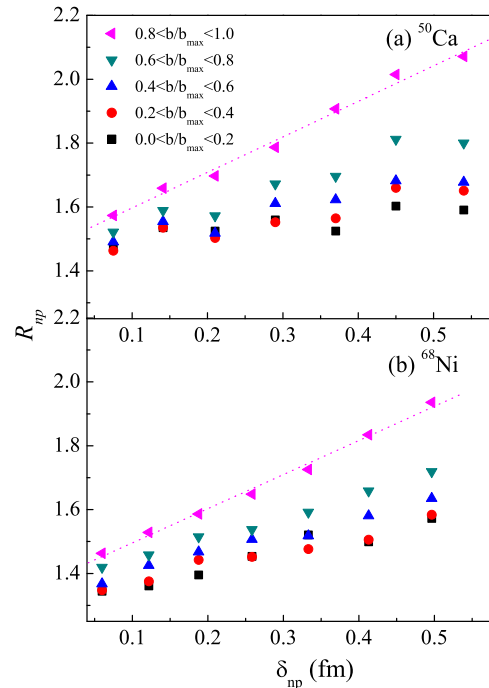


Figure 2: (Color online.) The dependence of R_{np} on neutron skin thickness of the projectile for $^{50}\text{Ca}+^{12}\text{C}$ (a) and $^{68}\text{Ni}+^{12}\text{C}$ (b) at 50A MeV under the condition of $Y > 0$. Different symbols are used for different range of the reduced impact parameter as shown in the legend. The dotted lines just guide the eye.

To avoid taking an unstable initialization of projectile and target in the IQMD calculation, we only select the initialization samples of those nuclei that meet the required stability conditions. The binding energies and root mean square (rms) radii of the initial configuration for the colliding nuclei are required to be stable. Using the selected initialization phase space of nuclei in IQMD to simulate the collisions, the nuclear fragments are constructed by a modified isospin-dependent coalescence model, in which nucleons with relative momentum smaller than $P_0 = 300$ MeV/c and relative distance smaller than $R_0 = 3.5$ fm will be combined into a cluster.

The collision processes of some Ca and Ni isotopes with ^{12}C target at 50A MeV are simulated using the IQMD model. The fragments including neutrons and

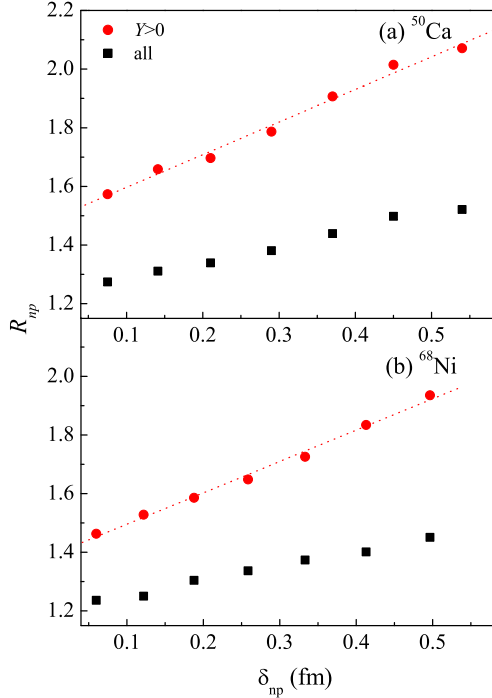


Figure 3: (Color online.) The dependence of R_{np} on neutron skin thickness under the condition of reduced impact parameter from 0.8 to 1.0 for $^{50}\text{Ca}+^{12}\text{C}$ (a) and $^{68}\text{Ni}+^{12}\text{C}$ (b) at 50A MeV. The results without any gate on the rapidity (Y) are shown as solid squares. The results with $Y > 0$ are plotted as solid circles. The dotted lines just guide the eye.

protons that formed during the evolution of the collision are constructed by the coalescence method. The yield ratio R_{np} of the emitted neutrons and protons can be calculated from the yields of the produced neutrons and protons. By changing the factor f_n in the neutron density distribution of the Droplet model for the projectile, different values of δ_{np} and the corresponding R_{np} are obtained. Thus we can obtain the correlation between R_{np} and δ_{np} . In the calculation, the time evolution of the dynamical process was simulated until $t = 200$ fm/c. The calculated R_{np} is stable after 150 fm/c as shown in Fig. 1, so we accumulate the emitted neutrons and protons between 150 fm/c and 200 fm/c in order to improve statistics. The R_{np} from different range of the reduced impact parameter for $^{50}\text{Ca}+^{12}\text{C}$ and $^{68}\text{Ni}+^{12}\text{C}$ are

plotted in Fig. 2. The reduced impact parameter is defined as b/b_{max} with b_{max} being the maximum impact parameter. From Fig. 2, we can see that R_{np} rises as δ_{np} increases. With δ_{np} being fixed, R_{np} also becomes larger with the increasing of the reduced impact parameter. It means that R_{np} from peripheral collisions is usually larger than that from central collisions. The main purpose of the present study is to investigate the relationship between R_{np} and the neutron skin thickness of the projectile. In order to minimize the target effect on R_{np} , we use rapidity (Y) cut to select neutrons and protons from the projectile. The rapidity of the fragment which is normalized to the incident projectile rapidity is defined as:

$$Y = \frac{1}{2} \log\left(\frac{E + p_z}{E - p_z}\right) / Y_{\text{proj}}, \quad (7)$$

where E is the energy of the fragment, p_z is the momentum of z direction, Y_{proj} is the rapidity of the projectile. We choose $Y > 0$ to strip away fragments coming from the target. From the results shown in Fig. 3, we can see that R_{np} with $Y > 0$ are larger than R_{np} without Y cut. Since the projectile is neutron-rich nucleus, the correlation between R_{np} and δ_{np} is stronger for nucleons coming from the projectile than those from both the projectile and target.

Strong linear correlation between R_{np} and δ_{np} of the projectile, especially for $0.8 < b/b_{\text{max}} < 1.0$, is exhibited in Fig. 2. It indicates that R_{np} is very sensitive to δ_{np} of the projectile, especially in peripheral collisions. For systematic study, reactions of other Ca and Ni isotopes such as $^{52,54,56}\text{Ca}$ and $^{60,62,64,66,70}\text{Ni}$ are also calculated. The results with the reduced impact parameter from 0.8 to 1.0 and the rapidity being positive are shown in Fig. 4. Strong linear relationship between R_{np} and δ_{np} are also observed for all projectiles. From Fig. 4, a linear function ($R_{np} = a + b \cdot \delta_{np}$) can describe the correlation between R_{np} and δ_{np} well for both Ca and Ni isotopes. The dependence between R_{np} and δ_{np} is fitted using this linear function. The mean slopes for Ca and Ni isotopes are 1.06 and 0.83, respectively.

From the above discussions, R_{np} could be viewed as a sensitive observable of δ_{np} for the projectile. If the produced neutrons and protons are measured by experiment, it is possible to extract δ_{np} from the

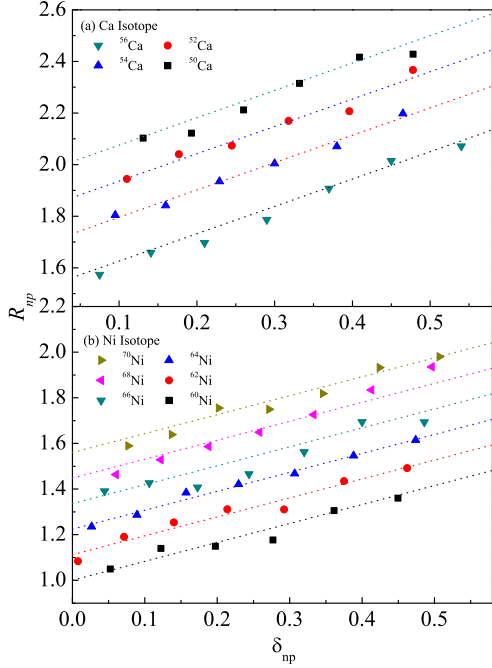


Figure 4: (Color online.) The dependence of R_{np} on neutron skin thickness under the condition of $Y > 0$ and $0.8 < b/b_{\max} < 1.0$ for $^{50,52,54,56}\text{Ca}+^{12}\text{C}$ (a) and $^{60,62,64,66,70}\text{Ni}+^{12}\text{C}$ (b) at 50A MeV. Different symbols are used for different projectile as shown in the legend. The dotted lines just guide the eye, for detail see text.

neutron-to-proton yield ratio R_{np} . From the fitted slope values, the estimated error of δ_{np} may be less than 0.08 fm if the uncertainty of R_{np} is less than 5%. It should be pointed out that this uncertainty does not take into account the error arising from the determination of impact parameter, which is always an important issue in studies of nuclear reactions in the energy range of our calculation. We estimate the uncertainty of δ_{np} for $0.6 < b/b_{\max} < 1.0$ to be around 0.1 fm when the uncertainty of R_{np} is 5%. To achieve high resolution, well defined experimental determination of the centrality of the reaction is required for this method.

In our calculation, different δ_{np} is obtained by changing the factor f_n in Eq.(3). We can also study the mass dependence of R_{np} with the same f_n as shown in Fig. 5. For $f_n = 1.0$, it refers to the neu-

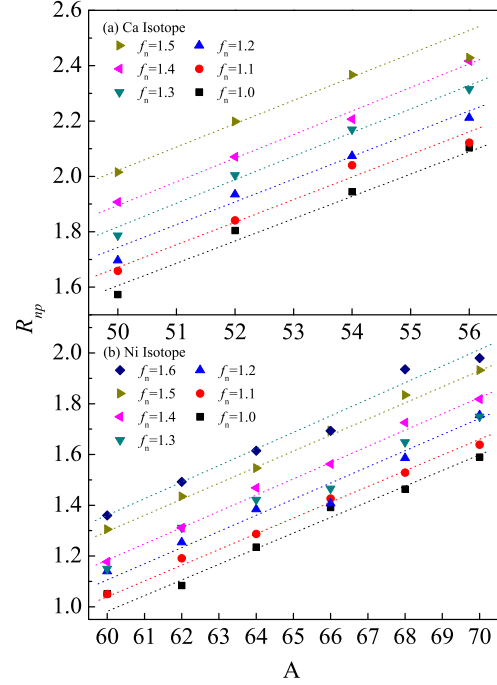


Figure 5: (Color online.) The dependence of R_{np} on the mass number A under the condition of $Y > 0$ and $0.8 < b/b_{\max} < 1.0$ for $^{50,52,54,56}\text{Ca}+^{12}\text{C}$ and $^{60,62,64,66,70}\text{Ni}+^{12}\text{C}$ at 50A MeV. Different symbols are used for different value of the factor f_n as shown in the legend. The dotted lines just guide the eye, for detail see text.

tron skin thickness of the Droplet model's prediction. In this figure, the linear dependence of R_{np} with the mass number A is also seen at different value of f_n . Due to the acceptance and efficiency in measurement of the emitted neutron and proton, the uncertainty of R_{np} may be not easy to be estimated which makes it difficult to obtain the error of δ_{np} . There is one method to minimize these effects: we can measure R_{np} of one isotope chain with different mass number. In this case, the acceptance and efficiency of neutron and proton will not change the mass dependence of R_{np} . If δ_{np} of some nuclei is larger than the normal value of the Droplet model, it will deviate from the line of $f_n = 1.0$. By studying the mass dependence of R_{np} , it is possible to extract δ_{np} and identify nucleus with abnormal neutron skin thickness.

The neutron excess ($I = (N - Z)/A$) dependence of

neutron skin thickness for four parameter sets (NL3, NL-SH, SkM*, SIII) in the Droplet model and self-consistent extended Thomas-Fermi (ETF) calculations have been investigated by Warda *et al.* [30]. Differences of the neutron skin thickness among different predictions increase with the increase of I . To distinguish which potential parameter set or method is more close to the experimental data, higher resolution measurement on neutron skin thickness is required for stable nuclei having small I in comparison with nuclei far from the stability line having large I value. From their results, the neutron skin thickness by different calculation varies from 0.01 fm to 0.11 fm at $I = 0.11$. In this sense, it will be capable of distinguishing different theoretical predictions when $I > 0.11$ by extracting δ_{np} from R_{np} measurement which the present paper proposes. In other words, the present method will be more feasible for heavy nuclei or intermediate mass nuclei far from the β -stability line.

In summary, we have made calculation on the relationship between R_{np} and the neutron skin thickness for the first time. The simulated data for Ca and Ni isotopes induced reactions show a good linear correlation between R_{np} and δ_{np} for neutron-rich projectile. It is suggested that R_{np} could be used as an experimental observable to extract the neutron skin thickness for neutron-rich nucleus. When the neutron skin thickness of one isotope is obtained, we can get some information on the EOS in different theoretical models such as Skyrme Hartree-Fock, relativistic mean-field and BUU model. From the isotope dependence of neutron skin thickness, a lot of information on the derivation of volume and surface symmetry energy, as well as nuclear incompressibility with respect to density can be extracted. This is very important to the study of the EOS of asymmetric nuclear matter.

Acknowledgments

This work is supported by National Natural Science Foundation of China under contract No.s 10775168, 10775167, 10979074 and 10747163, Major State Basic Research Development Program in China

under contract No. 2007CB815004, Knowledge Innovation Project of Chinese Academy of Sciences under contract No. KJCX3.SYW.N2, and the Shanghai Development Foundation for Science and Technology under contract No. 09JC1416800.

References

- [1] G. Fricke, C. Bernhardt, K. Heilig, L. A. Schaller, L. Schellenberg, E. B. Shera, C. W. DeJager, *At. Data Nucl. Data Tables* 60 (1995) 177.
- [2] L. Ray, G. W. Hoffmann, W. R. Coker, *Phys. Rep.* 212 (1992) 223.
- [3] C. J. Horowitz, S. J. Pollock, P. A. Souder, R. Michaels, *Phys. Rev. C* 63 (2001) 025501.
- [4] P. Danielewicz, *Nucl. Phys. A* 727 (2005) 233.
- [5] M. Centelles, X. Roca-Maza, X. Viñas, M. Warda, *Phys. Rev. Lett.* 102 (2009) 122502.
- [6] A. Klimkiewicz, N. Paar, P. Adrich, M. Falot, K. Boretzky, T. Aumann, D. Cortina-Gil, U. DattaPramanik, Th. W. Elze, H. Emling, H. Geissel, M. Hellström, K. L. Jones, J. V. Kratz, R. Kulesa, C. Nociforo, R. Palit, H. Simon, G. Surówka, K. Sümmerer, D. Vretenar, W. Waluś, *Phys. Rev. C* 76 (2007) 051603(R).
- [7] L. W. Chen, C. M. Ko, B. A. Li, *Phys. Rev. C* 72 (2005) 064309.
- [8] B. A. Brown, *Phys. Rev. Lett.* 85 (2000) 5296.
- [9] S. Yoshida and H. Sagawa, *Phys. Rev. C* 69 (2004) 024318.
- [10] T. Suzuki, H. Geissel, O. Bochkarev, L. Chulkov, M. Golovkov, N. Fukunishi, D. Hirata, H. Irnich, Z. Janas, H. Keller, T. Kobayashi, G. Kraus, G. Münzenberg, S. Neumaier, F. Nickel, A. Ozawa, A. Piechaczek, E. Roeckl, W. Schwab, K. Sümmerer, K. Yoshida, I. Tanihata, *Nucl. Phys. A* 630 (1998) 661.
- [11] F. Sammarruca, P. Liu, *Phys. Rev. C* 79 (2009) 057301.

- [12] M. Liu, N. Wang, Z. X. Li, X. Z. Wu, Chin. Phys. Lett. 23 (2006) 804.
- [13] A. Bhagwat, Y. K. Gambhir, Phys. Rev. C 73 (2006) 054601.
- [14] Y. G. Ma, W. Q. Shen, J. Feng, Y. Q. Ma, Phys. Lett. B 302 (1993) 386.
- [15] Y. G. Ma, W. Q. Shen, J. Feng, Y. Q. Ma, Phys. Rev. C 48 (1993) 850.
- [16] X. Z. Cai, W. Q. Shen, J. Feng, D. Q. Fang, Y. G. Ma, Q. M. Su, H. Y. Zhang, P. Y. Hu, Chin. Phys. Lett., 17 (2000) 565.
- [17] W. D. Myers, W. J. Swiatecki, Ann. Phys. A 84 (1974) 186;
W. D. Myers and W. J. Swiatecki, Nucl. Phys. A 336 (1979) 267.
- [18] T. Suzuki, H. Geissel, O. Bochkarev, L. Chulkov, M. Golovkov, D. Hirata, H. Irnich, Z. Janas, H. Keller, T. Kobayashi, G. Kraus, G. Mnzenberg, S. Neumaier, F. Nickel, A. Ozawa, A. Piechaczek, E. Roeckl, W. Schwab, K. Smererer, K. Yoshida, I. Tanihata, Phys. Rev. Lett. 75 (1995) 3241.
- [19] C. W. Ma, Y. Fu, D. Q. Fang, Y. G. Ma, X. Z. Cai, W. Guo, W. D. Tian, H. W. Wang, Chin. Phys. 17 (2008) 1216.
- [20] M. A. Famiano, T. Liu, W. G. Lynch, M. Mocko, A. M. Rogers, M. B. Tsang, M. S. Wallace, R. J. Charity, S. Komarov, D. G. Sarantites, L. G. Sobotka, G. Verde, Phys. Rev. Lett. 97 (2006) 052701.
- [21] Y. G. Ma, Q. M. Su, W. Q. Shen, D. D. Han, J. S. Wang, X. Z. Cai, D. Q. Fang, H. Y. Zhang, Phys. Rev. C 60 (1999) 024607.
- [22] Y. X. Zhang, P. Danielewicz, M. Famiano, Z. X. Li, W. G. Lynch, M. B. Tsang, Phys. Lett. B 664 (2008) 145.
- [23] M. B. Tsang, Y. X. Zhang, P. Danielewicz, M. Famiano, Z. X. Li, W. G. Lynch, A. W. Steiner, Phys. Rev. Lett. 102 (2009) 122701.
- [24] B. A. Li, L. W. Chen, G. C. Yong, W. Zuo, Phys. Lett. B 634 (2006) 378.
- [25] J. Rizzo, M. Colonna, M. Di Toro, Phys. Rev. C 72 (2005) 064609.
- [26] J. Aichelin, A. Rosenhauer, G. Peilert, H. Stoecker, W. Greiner, Phys. Rev. Lett. 58 (1987) 1926.
- [27] J. Aichelin, Phys. Rep. 202 (1991) 233.
- [28] W. D. Myers, K. H. Schmidt, Nucl. Phys. A 410 (1983) 61.
- [29] A. Trzcińska, J. Jastrzebski, P. Lubiniński, F. J. Hartmann, R. Schmidt, T. V. Edigy, B. Klos, Phys. Rev. Lett. 87 (2001) 082501.
- [30] M. Warda, X. Viñas, X. Roca-Maza, M. Centelles, Phys. Rev. C 80 (2009) 024316.